Testing and Commissioning of a Low-Speed Wind Tunnel (LSWT) Test Section

Dr. Ihssan Y. Hussain
Professor
College of Engineering – University of Baghdad
email:drihsan@uobaghdad.edu.iq
dr.ihsanyahya1@yahoo.com

Anmar Hamid Ali
Lecturer
College of Engineering – University of Baghdad
email:aha_has@yahoo.com

ABSTRACT

The calibration of a low-speed wind tunnel (LSWT) test section had been made in the present work. The tunnel was designed and constructed at the Aerodynamics Lab. in the Mechanical Engineering Department/University of Baghdad. The test section design speed is 70 m/s. Frictional loses and uniformity of the flow inside the test section had been tested and calibrated based on the British standards for flow inside ducts and conduits. Pitot-static tube, boundary layer Pitot tube were the main instruments which were used in the present work to measure the flow characteristics with emphasize on the velocity uniformity and boundary layer growth along the walls of the test section. It is found that the maximum calibrated velocity for empty test section is 55 m/s. Three speeds are tested for uniformity and walls boundary layer at inlet and mid-section of test section. The results show that the flows are uniform at inlet and mid-section with turbulent flow from inlet to outlet.

Key words: Wind Tunnel, Test Section Calibration, Turbulent Flow

معايرة مقطع اختبار لنفق هوائي واطيء السرعة

أ.د.أحسان يحيى حسين
قسم الهندسة الميكانيكية
كلية الهندسة / جامعة بغداد

نمارحامد علي
قسم الهندسة الميكانيكية
كلية الهندسة / جامعة بغداد

الخلاصة

في هذا العمل تمت معايرة مقطع اختبار لنفق هوائي واطيء السرعة. تم تصميم وتركيب النفق (في عمل سابق) في مختبر الهوائيات بقسم الهندسة الميكانيكية-جامعة بغداد. السرعة التصميمية لمقطع الاختبار هي 70 م\ثا. تم اختبار ومعايرة الخسائر الاحتكاكية والتجانس للجريان داخل مقطع الاختبار بالاعتماد على المواصفات البريطانية للجريان داخل الانابيب والانفاق. انبوب Pitot-static, وانبوب Pitot للطبقة المتاخمة استخدما كوسائل رئيسة في البحث الحالي لقياس خواص الجريان مع التشديد على تجانس السرعة وتنامي الطبقة المتاخمة لجدران مقطع الاختبار. تم معايرة السرعة القصوى لمقطع الاختبار وهو فرغ وقد كانت 55 م\ثا. ثلاث سرع تم اختبارها لقياس التجانس والطبقة المتاخمة للجدران عند الدخول والمقطع النصفي لمقطع الاختبار. النتائج اظهرت ان الجريان منتظم عند الدخول والمقطع النصفي بجريان مضطرب من المدخل حتى المخرج.

1. INTRODUCTION

Wind tunnel is rapid, economical and accurate mean for conducting aerodynamic researches and obtaining aerodynamic data to support design decisions. There is a considerable and growing volume of aerodynamic research in the development of aircrafts, automobiles, marine's vehicles, and architectural structures. The first step in the design of a tunnel is to determine the shape and size of test section based on the intended use of the facility. The test section size, speed and design will determine the required power. The overall aerodynamic objective for most wind tunnels is to obtain a flow in the test section that is as near as possible to a parallel steady flow with uniform speed throughout the test section. **Swanson and Gillis 1944,** had shown three categories of flow non-uniformities, these were the airspeed change along longitudinal and vertical axis of the tunnel and variation of the air-flow angle in the region of model. Calibrations were made by surveying the flow over the plane perpendicular and parallel to the airstream at the position to be occupied by the model. Pitch, yaw and Pitot-static tube with manometers measuring static, total and air flow angularity. **Pope 1961** had discussed the air-flow measuring instruments and presented the data obtained when calibrating low-speed, and high speed wind tunnels. The methods for the measurement of flow in pipes and ducts are illustrated in the **British Standards (BS 1042) 1968.** Pressure losses associated with tunnel geometry, flow irregularities and boundary layer growth mean that the pressure difference measured by the pitot tubes may not accurately represent the true dynamic pressure within the tunnel test section **Edwards 2000**. A new longer test section and contraction installation produced a thicker boundary layer on the test section walls and then increased the air velocity along test section. The wind velocity in the test section of the Low Speed Wind Tunnel (LSWT) at the Mechanical Engineering Department of university of Baghdad is obtained from pressure measurements using pitot tubes located at the entrance and mid section of the tunnel test section. Static pressure and velocity distributions in the wind tunnel test section have been investigated mainly with the objective of determining the static pressure gradient in the test section so that buoyancy corrections should be made for models. The recent installation of a new test section for LSWT has made it necessary to perform tests to determine a new calibration. Pressure data was acquired from standard pitot probe at various positions within the tunnel test section over a large velocity range.

2. LOW SPEED WIND TUNNEL DESCRIPTION

An open circuit wind tunnel was designed and constructed, **Hussain et al., 2011**. The assembled wind tunnel is shown in **Fig. 1** which shows dimensions and components. A brief description of the tunnel components are given below.

2.1 Contraction Section and Settling Chamber

The contraction section and settling chamber were made of steel sheets and both have rectangular cross section. A contraction ratio of 8.94:1 is used in the equations discussed in **Hussain and et. al. 2011** at the Mechanical Engineering / University of Baghdad. The settling chamber contains three screens and is connected to the bell mouth at the inlet and contraction inlet at the exit section. The contraction section is joined to the test section by a mating flange.

2.2 Test Section

The test section of (0.7 m x 0.7 m) was designed to be suitable size for different models sizes. The wood thickness of (30 mm) is used to prevent wall curvature due to suction or negative gage pressure inside test section. The test section also provides with Plexiglas window on one side of the test section to allow viewing the model setting inside wind tunnel. A square cross section as shown in **Fig. 1** is chosen with constant taper of right and left walls to prevent the effect of boundary layer growth along walls (buoyancy effect). The test section is supported with flanges at either ends of the sections for fastening with other sections.

2.3 Diffuser

The diffuser is made of steel sheets and it is used to connect the test section with the fan housing by converting the square cross section of 700 mm at diffuser inlet plane to circular cross section at exit plane of 1500 mm. The length of diffuser is 6000 m as shown in **Fig. 1**. Rubbers are used to reduce vibration and provide an air tight seal between sections. A coarse screen is fixed to protect the fan from damage.

2.4 Power Plant

Axial flow fan driven by a 75hp, AC current motor of 3000 rpm is used to provide the power to overcome the pressure loses along the tunnel sections. The axial fan is mounted on the fan housing and fixed by bolts on the ground. The motor speed control is from zero to 3000 rpm, a control unit is used to give increments to the motor rotation from zero to max speed of rotation.

3. EXPERIMENTAL EQUIPMENT

3.1 Pitot Tube

The **British Standards** Pitot tube or as called boundary layer Pitot tube is shown in **Fig. 2-a** which is made from stainless steel tube of (4.5 mm) outer diameter and (415 mm) in the overall length. The head of hypodermic tubing is (1 mm) diameter. This instrument is used to measure the total pressure at the test section. The boundary layer velocity profile is measured using Pitot-tube with static tube to measure the dynamic pressure through layer. This pitot tube is also used to measure the boundary layer thickness, by traversing it through the boundary layer and normal to the wall, until reaching to maximum reading. Then, the distance travelled by the tube relative to the wall, which is arbitrary, represents the boundary layer thickness. The distance read from the ruler is fixed on the traversing mechanism.

3.2 Static Tube

The static tube is used to measure the static pressure of the flow. It consists of a steel tube (2.4 mm) outer diameter, with head sealed by soldering and finished to take a hemisphere nose as shown in **Fig. 2-b**. Four static holes of (0.5 mm) diameter and (19.5 mm) away from the blocked end are made to measure the pressure. The (2.4 mm) tube is joined to a (4.5 mm) diameter copper tube. The static tube is fixed perpendicular to the x-y plane and used with Pitot tube to measure the dynamic pressure of boundary layer.

3.3 The Pitot - static tube

This instrument is used to measure the dynamic, total and static pressures of the non-viscous flow at the centre of the wind tunnel test section for three speeds of the tunnel. These values were used during the calibration of the wind tunnel. The Pitot static tube is mounted

co-axially, with the Pitot tube inside the static tube. It consists of a stainless steel tube (5 mm) outer diameter with a blunt nose; the four static holes are (0.5 mm) diameter and (30 mm) away from the nose. The diameter of the Pitot tube is (1 mm). **Fig. 2-c** shows the details of the Pitot-Staic tube.

3.4 The Micro Manometer

The Dwyer Series 475 Mark III Handheld Digital Manometer is ideal for field calibration, monitoring or trouble shooting HVAC systems, clean rooms or a wide range of other low pressure pneumatic systems. This handy instrument measures positive, negative or differential pressures of air and natural gases in ranges from (0.249 kPa) to (10.34 bar). Dual push pads on the front panel control on-off, auto zero, and pressure unit selection were provided as shown in **Fig. 2-d**. The device was calibrated with total error reading percentage of 0.6% by **the Iraq central organization for standardization and quality control**.

3.5 Traversing Mechanism

In order to carry out the measurements at various stations inside the test section, a vertical traverse unit was manufactured specially to fix and move the instruments vertically using DC motor connected to a slide plate with upward and downward movement of the instruments as shown in **Fig. 2-e**. A controller unit is used with push buttons to move the instrument accurately to a specified position. Side ruler was used to measure the vertical movement of the slide part of the traversing mechanism.

4. EXPERIMENTAL PROCEDURES

The following experimental procedures were followed in the present work:

1- The laboratory were prepared for the experiment specially stagnation pressure by opening all doors and windows to the atmosphere.

2- The measuring tubes were mounted in the traversing mechanisms and adjusted for measuring.

3- The connection between the measuring tubes and micro manometer were made by a P.V.C tubes.

4- The micro manometer was operated and adjusted to the desired unit.

5- The fan was then adjusted to give the desired speed using controlling unit. In the present work (10, 30 and 45 m/s)

6- (10-15) minutes were allowed for the rig to reach the steady state.

7- The laboratory temperature was recorded at the beginning and end of the experiment. The maximum temperature variation detected was (3^{o} C).

4.1 Total Mean Velocity

The total mean velocity of the flow inside the test section could be measured using Pitot static tube at the centre of the square shape cross section. The Cartesian coordinates are illustrated in the **Fig. 3** for the inlet or mid plane of the test section. The coordinate will be reliable for all calibration tests.

4.2 Experimental Grid Arrangement

To calibrate the test section flow uniformity, two planes are selected for this calibration, the first one at inlet plane and the other at model mounting position (middle plane). These sections are discretized into grid points as shown in **Fig. 3** as recommended by **Hussain 1989** depending on the **British Standards 1968** for the calibration flow inside

conduits and tunnels. The points are distributed as shown in **Fig. 3** near the walls to survey boundary layer effects. To measure the dynamic pressure at each point, Pitot tubes are mounted to the traverse system to move vertically at each row points beginning from lower surface to the upper surface depending on the ruler fixed on the traverse unit.

4.3 Longitudinal Static Pressure Measurements

The buoyancy effect along the test section must be measured using static tube with micro manometer. The static pressure along the test section centre line was measured at four positions along the test section.

5. DATA PROCESSING

5.1 Total Mean Velocity

The local mean velocity at the test section and at the boundary layer was calculated from the measured dynamic pressure, which is the difference between the total pressure and the static pressure;

$$V = \sqrt{\frac{\Delta P}{0.5 * \rho_\infty}} \tag{1}$$

Where ΔP is the dynamic pressure measured by micro-manometer in (Pa), and ρ_∞ is the density calculated from a barometric pressure measurement, a test section static pressure measurement relative to the atmosphere and a test section temperature determination along with the equation of state. From the manual book of the pitot tube device, the density could be found from the following equations;

$$\rho_\infty = 1.325 \times P_B T \tag{2}$$

where P_B is the barometric pressure in inches of mercury. T is the absolute temperature (indicated temperature in ^oF plus 460).

For standard sea level air properties,

$$V = \sqrt{\frac{\Delta P}{0.5 * 1.225}} = 40.406 * \sqrt{\Delta P} \tag{3}$$

5.2 Boundary Layer Characteristics

The wall boundary layer velocity profile could be measured and fitted with power law function to find the boundary layer characteristics as displacement thickness, momentum thickness and shape function using Simpson's 1/3 Rule for equal interval in the y-direction. These characteristics may be defined as follows;

$$\delta^* = \int_0^\delta \left(1 - \left(\frac{U}{U_e}\right)\right) dy \tag{4}$$

$$\theta = \int_0^\delta \left(1 - \left(\frac{U}{U_e}\right)\right)\left(\frac{U}{U_e}\right) dy \tag{5}$$

$$H = \frac{\delta^*}{\theta} \tag{6}$$

Where U/U_e is the velocity profile of the flow near the tunnel wall at specified position.

5.3 Velocity Error Analysis

The local mean-velocity (V) was given by equation;

$$V = cc\sqrt{h} \quad (7)$$

where cc is constant depends on the equation (1) parameters. Thus, to find the relative error, it will be differentiated logarithmically, then;

$$\frac{dV}{V} = \frac{1}{2} \times \frac{dh}{h} \quad (8)$$

where (dh) is the absolute error in the dynamic pressure head, and it is calculated as;

$$dh = \sqrt{((h - h_m)^2 + (\delta h)^2)} \quad (9)$$

The first term in the R.H.S of equation (9) represents the deviation from the mean (h_m) of all measured values of (h), and it is calculated as ($\frac{\sum_{i=1}^{n} h_i - h_m}{n}$), where (n) is the number of points, where as the second term represents the error of the measurements.

As example, the error in the velocity 30 m/s at the test section inlet without the model as presented in are calculated using the measured values of the dynamic pressure head at the mesh points where the mean value h_m is (55.56138 mmH2O), and deviation from the mean was (0.824093 mmH2O). The error of measurements was taken as (0.5 mmH2O). Hence, from equation (9), the absolute error (dh) was calculated as (0.96391mmH2O), thus, from Eq. (8), the velocity relative error will be (± 0.8674%).

6. CFD SIMULATION

A three dimensional flow had been simulated using COMSOL 3.5 commercial programme. Turbulent flow with κ-ω turbulence model was used to simulate the flow inside wind tunnel. Three velocities were simulated and presented to study the flow characteristics and behaviour through the test section. The simulation may be represented with the boundary conditions illustrated in **Fig. 4** where the inlet velocity was measured from the wind tunnel inlet section using flow anemometer. Unstructured tetrahedral elements were used with total number of 12000 elements. **Fig. 5** shows a generated free mesh by the programme for the flow inside the wind tunnel. Stationary segregated solution method was used with tolerance 10^{-5} and the maximum numbers of iterations were 2000 step. The solutions were represented in to contours for the pressure and velocity distributions.

7. RESULTS AND DISCUSSIONS

The wind tunnel total velocity was calibrated and presented in **Fig. 6.** The Pitot static tube was fixed at the test section inlet plane to record the total mean velocity by using micro-manometer. The figure relates the input current to the fan with total velocity which is ranged from 0 to maximum speed. It is found that the velocity at the test section had maximum value of 55 m/s. The discrepancy in the designed and measured velocity may be attributed to the fan design blade.

As shown in **Fig. 7**, the uniformity distributions of the inlet velocity across the inlet plane of test section for 10, 30 and 45 m/s respectively are clearly flatten at the core section as expected. Small regions at the test section walls are shown to be distorted due to presence of boundary layer on the wall surface. The velocities 30 and 45 m/s show a deep valley at the centre of the section due to the wake of frontal Pitot-static tube which was fixed to measure

the inlet velocity. This Pitot must be removed from the inlet section after measuring the velocity to a specified value.

The mid section velocity uniformity is illustrated in **Fig. 8** for different inlet velocities of 10, 30, and 45 m/s respectively. The distributions are fair enough for different velocities and the discrepancies may be attributed to the corner stationary flows of the test section. The velocities distributions show an important behaviour at the centre regions, where the maximum values are distributed in the y-direction while no similar distribution are found in x-direction, this may be attributed to the divergence angle of the test section for the upper and lower surfaces which are tilted to prevent buoyancy effect along the test section.

Figs. 9, 10, 11, and **12** show velocity profiles at the inlet and mid planes of test section for horizontal and vertical centre axes. As shown the flows are flatten at the centre location except at the side walls where the boundary layer growth is the major influence to the uniformity of the test section and symmetrical distribution along the vertical and axial axis.

The velocity profiles along the diagonals of the inlet and mid planes are shown in **Figs. 13, 14, 15,** and **16.** It could be seen that, as the test section velocity increased the profiles became inflated slightly specially at velocity 30 m/s which may be attributed to the wall boundary layer effects on the core velocities.

It is important to find the velocity profiles across the boundary layer of the test section walls. Since the flow is symmetric across different axis as illustrated in the previous figures, the boundary layer on the lower surface is measured by finding a velocity profiles at the mid section for three velocities10, 30 and 45 m/s. As can be seen, turbulent velocity profiles are clearly appeared in **Figs. 17, 18** and **19**. A power low was used to find a curve fitting for the experimental data. Equations are shown in the figures, and good fittings are evaluated for the velocity profiles. The boundary layer characteristics (displacement thickness, momentum thickness) could be calculated for these profiles and are given in the **Table 1**. No boundary layer separations are obvious through test section walls. By assuming the boundary layer thickness is linear with distance. Taking the relation from **schlechting**, $\delta(x) = .37\, x \left(\frac{ux}{v}\right)^{\left(-\frac{1}{5}\right)}$, one obtains a boundary layer thickness of 20.8 mm for flow at the test section at velocity 10 m/s if the boundary layer begins at the inlet of the test section. The measured thickness for this velocity at mid section is 19 mm, which is good prediction to the boundary layer thickness. Most of results are shown in the **Table 1**. It could be noticed that the boundary layer thickness increased with increasing velocity which may be attributed to the traverse pressure gradient normal to the wall which increases the boundary thickness. Same thing may be noticed for momentum thicknesses and shape factor which give an indication for shear stress and frictional losses along the test section.

Figs. 20, 21, show the flow inside wind tunnel for inlet velocity equal to 1.23 m/s experimentally which gives 10 m/s at the test section. One notes that the pressure at the test section is under the atmospheric pressure with minus value and the velocity also equal to 10 m/s as measured experimentally. **Figs. 22, 23, 24,** and **25** have same distributions with inlet velocities 3.5 m/s for 30 m/s and 5.25 m/s for 45 m/s respectively.

The static pressure along test section is represented in **Fig. 26**. The figure shows a gradual decrement in the static pressure although it is small but could be represented as a linear behaviour for all three velocities. For velocity 30 m/s as example,

$$D = (p_{out} - p_{in}) * A = (-0.53 + 0.57) * 1000 * (0.7 * 0.7) = 19.6\ N$$

$$C_D = \frac{D}{0.5\rho_\infty {V_\infty}^2} = \frac{19.6}{0.5 * 1.23 * 30^2} = 0.035$$

The drag coefficient for the model inside test section must be corrected due to presence of the boundary layer growth along walls of test section. **Pope,1978,** presented a method for calculating buoyancy effects on the models inside test section. The static pressure gradient shrinking streamlines transiting down the test section. The squeezing effect accounted and added to the pressure gradient effect. The total drag increment with squeezing effect is;

$$\Delta D_B = -\frac{\pi}{2}\lambda\, t^2(\frac{dp}{dl})$$

where λ correction factor, and t is the body thickness.

8. CONCLUSION

The overall aerodynamic objectives for most wind tunnels is to obtain a flow in the test section that is as near as possible to a parallel steady flow with uniform speed throughout the test section. The wind velocity in the test section of the Low Speed Wind Tunnel (LSWT) at the Mechanical Department of university of Baghdad is obtained from pressure measurements using pitot tubes located at the entrance and mid section of the tunnel test section. The static pressure along the test section centre line was measured at four positions along the test section. The local mean velocity at the test section and at the boundary layer was calculated from the measured dynamic pressure. The inlet and mid plane of test section for 10, 30 and 45 m/s are clearly flatten at the core section. A power low was used to find a curve fitting for the experimental data of boundary layer on the lower surface, and good fittings are evaluated for the velocity profiles, which mean the flow is turbulent. The static pressure along the test section was a linear behaviour.

9. REFERENCES

- B. S., 1042, 1968.
- Edwards, C. D., 2000, *Calibration* of *the Reference Velocity in the Test Section of the Low-Speed Wind Tunnel at the Aeronautical and Maritime Research Laboratory,* DSTO-TN-0248
- Hussain, I. Y., Ali, A. H., Majeed, M. H., Sarsam, W. S., December 2011, *Design, Construction and Testing of Low-Speed Wind Tunnel with its Measurement and Inspection Devices,* Journal of Engineering, Vol. 17, No.6, p.p. 1550-1566.
- Hussain, I. Y., 1989, *Computational and Experimental Investigation of Three-Dimensional Turbulent Boundary-Layer,* M.Sc. thesis, University of Baghdad.
- Pope, A., 1961, *Wind Tunnel Calibration Techniqu,* AGARD-AG-54.
- Swanson, R. S., and Gillis, C. L., 1944, *Wind-Tunnel Calibration and Correction Procedures for Three-Dimensional Models*, NACA, ARR No.L4E31

NOMENCLATURE

ΔP	(P_o-P_∞)	Pa
C_D	drag coefficient	
D	drag force	N
D_B	buoyancy Drag	N
dp/dl	pressure gradient	Pa/m
H	shape factor	
P_∞	free stream Static pressure	Pa
P_o	total Pressure	Pa
t	body thickness	M
U	local velocity	m/s
U_e	boundary layer edge velocity	m/s
V	total mean velocity	m/s
δ	boundary layer edge	m
δ^*	boundary layer displacement thickness	m
θ	boundary layer momentum thickness	m
λ	correction factor	
ν	kinematic viscosity	m^2/s
ρ_∞	free stream density	m^3/kg

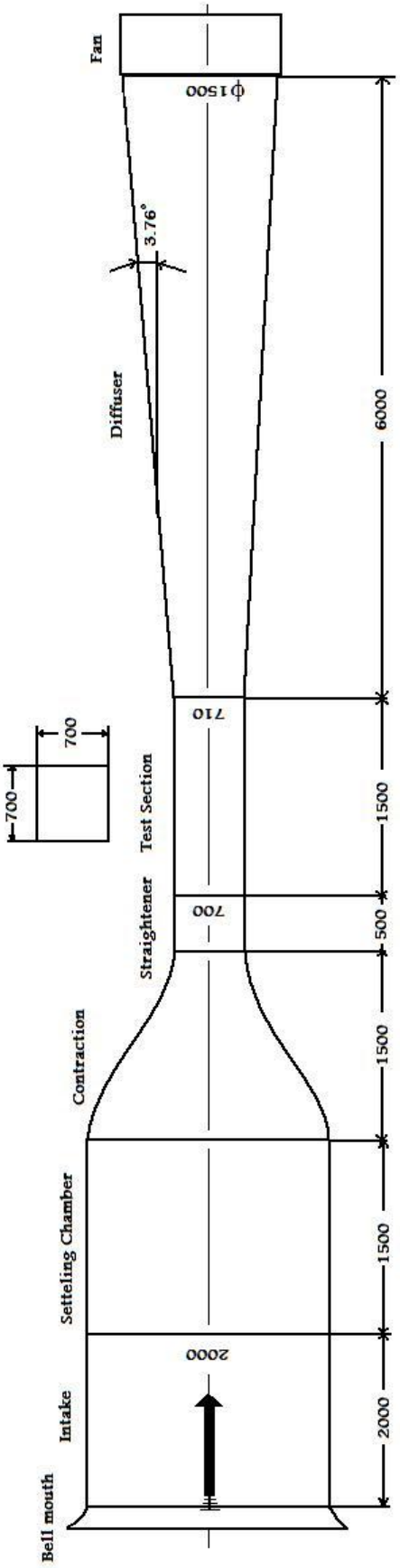

Figure 1. Wind tunnel dimensions (all are in mm).

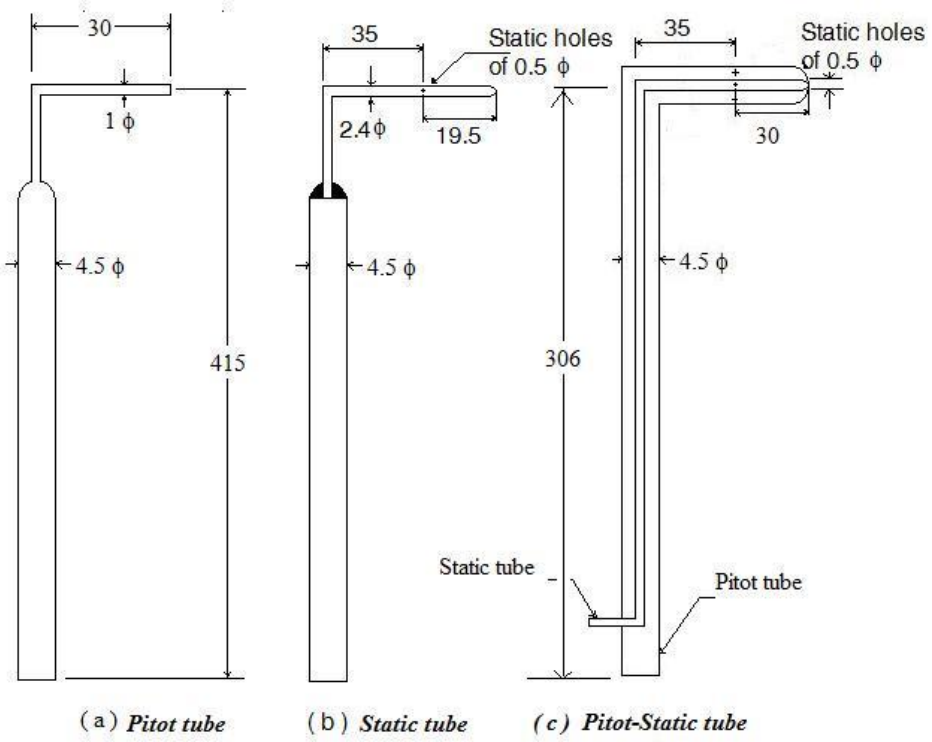

(d) Micro-manometer

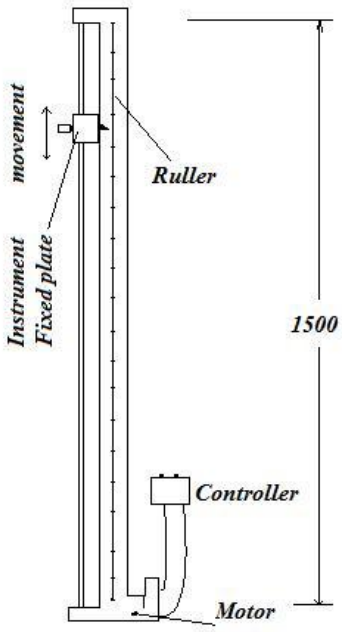

(e) Traverse system

Figure 2. Types of measurement instruments (all dimensions are in mm).

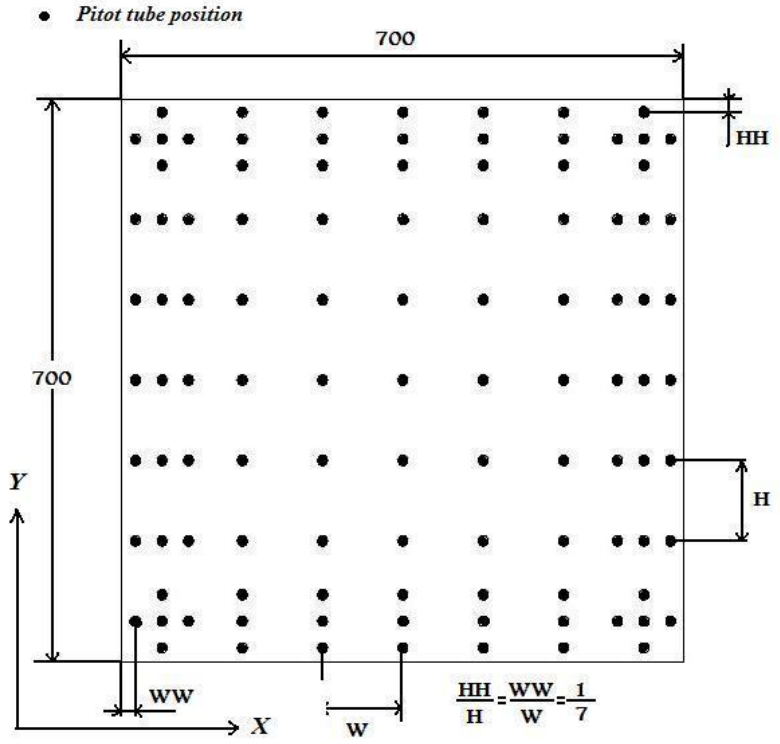

Figure 3. Mesh arrangement at the test section (all dimensions are in mm).

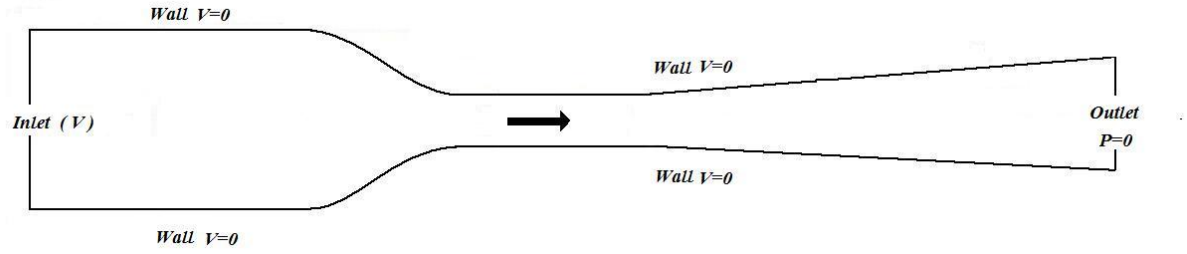

Figure 4. Wind tunnel CFD boundary conditions.

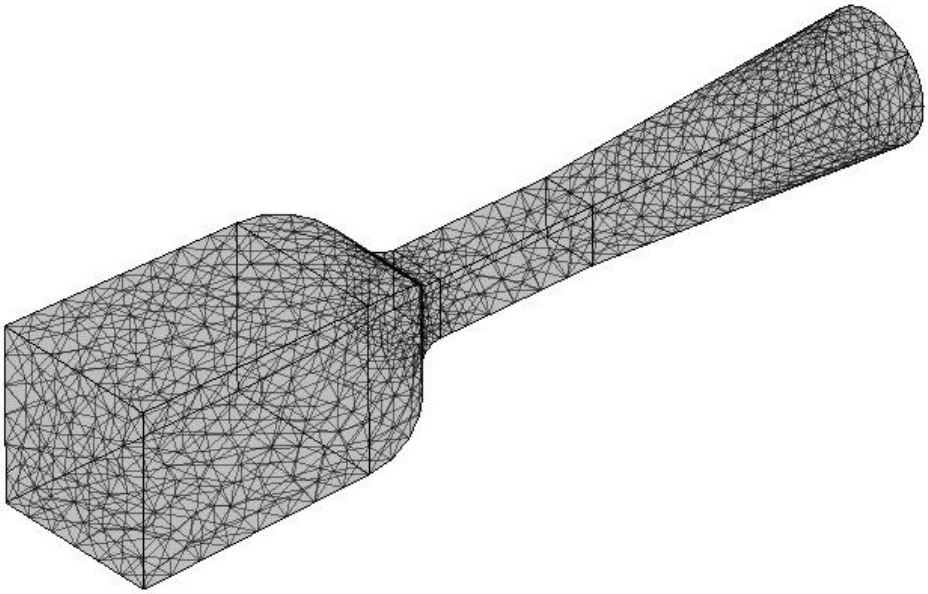

Figure 5. Wind tunnel descretization using COMSOL 3.5 program.

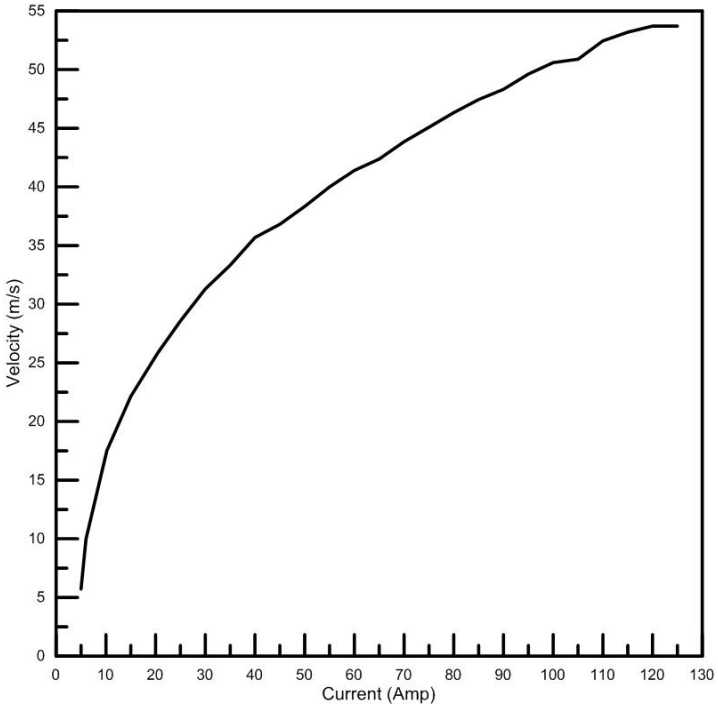

Figure 6. Total velocity as a function of the fan input current.

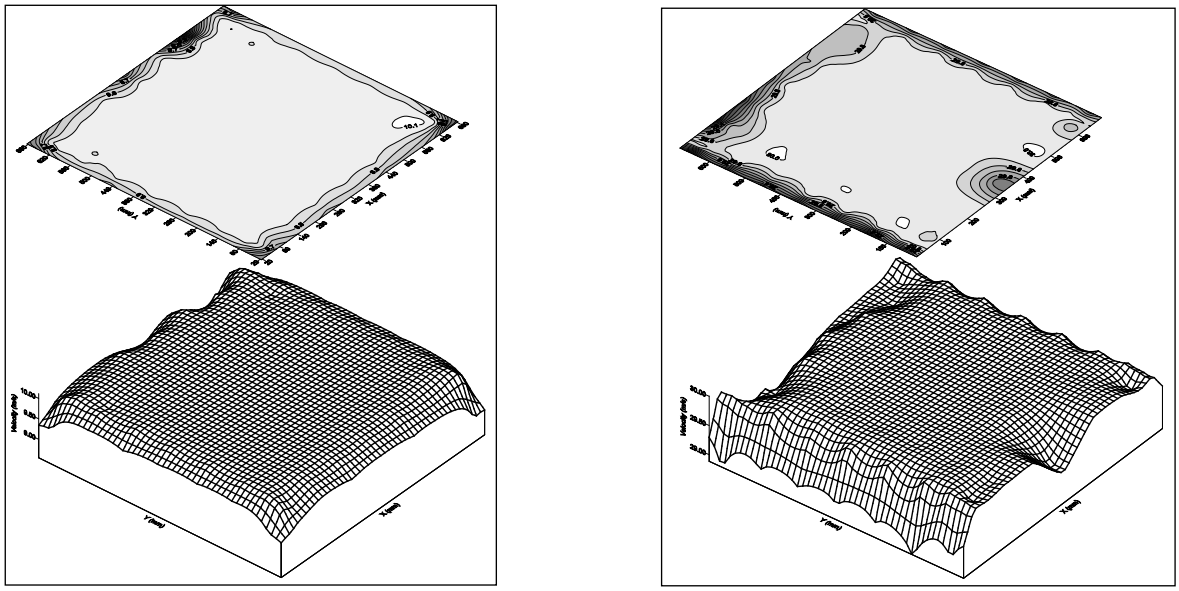

Velocity = 10 m/s

Velocity = 30 m/s

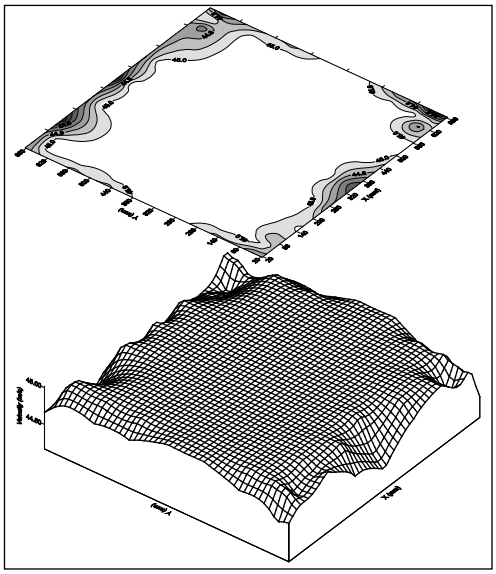

Velocity = 45 m/s

Figure 7. Velocity uniformity across the inlet plane of the test section for 10, 30, and 45 m/s.

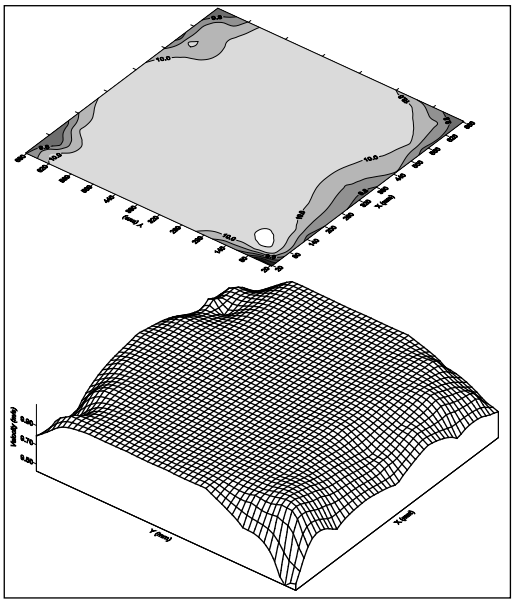

Velocity = 10 m/s

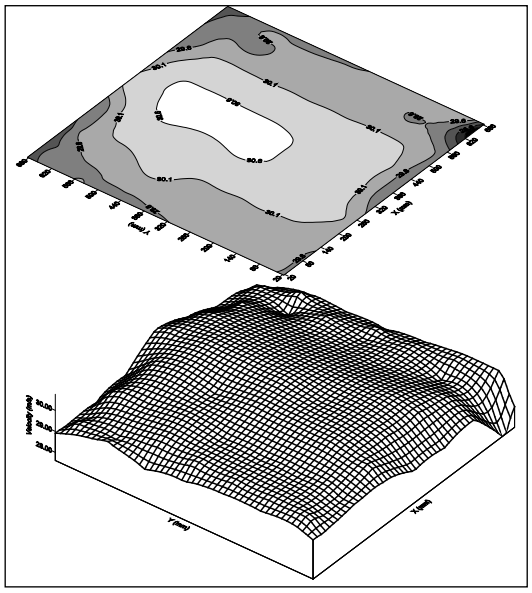

Velocity = 30 m/s

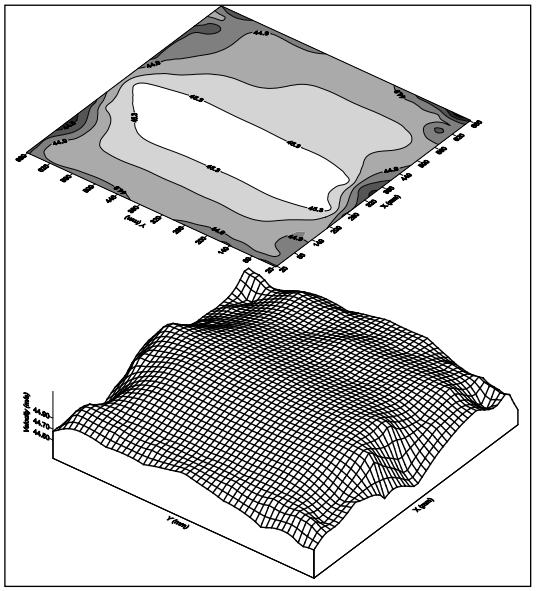

Velocity = 45 m/s

Figure 8. Velocity uniformity across the mid plane of the test section for 10, 30, and 45 m/s.

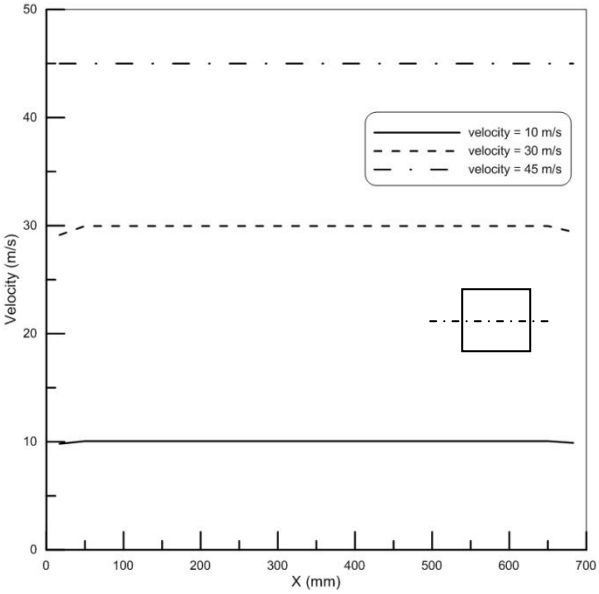

Figure 9. Test section velocity of the horizontal axis at the inlet plane.

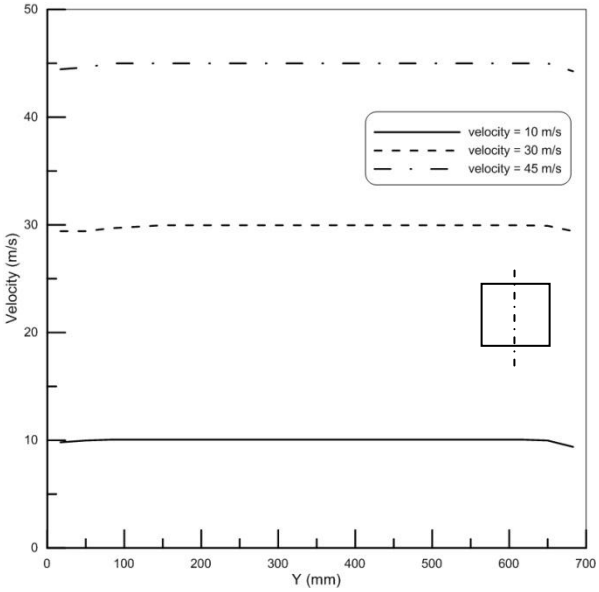

Figure 10. Test section velocity of the vertical axis at the inlet plane.

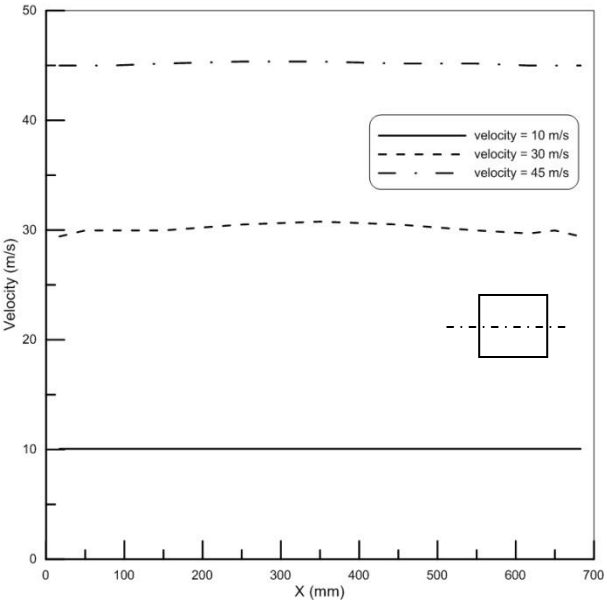

Figure 11. Test section velocity of the horizontal axis at the mid plane.

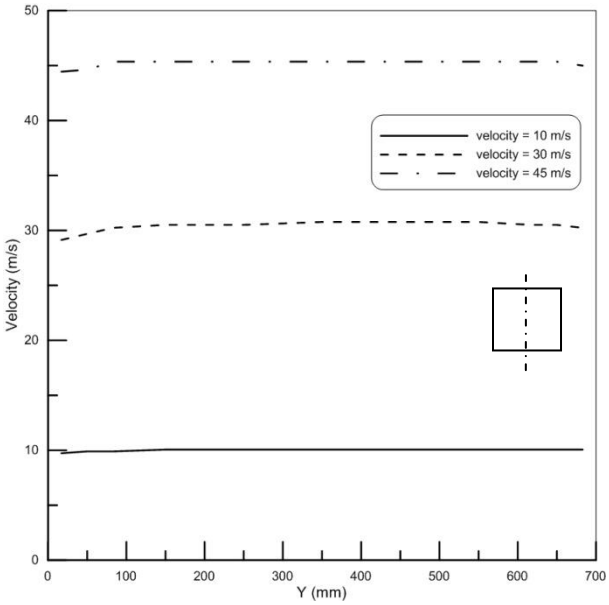

Figure 12. Test section velocity of the vertical axis at the mid plane.

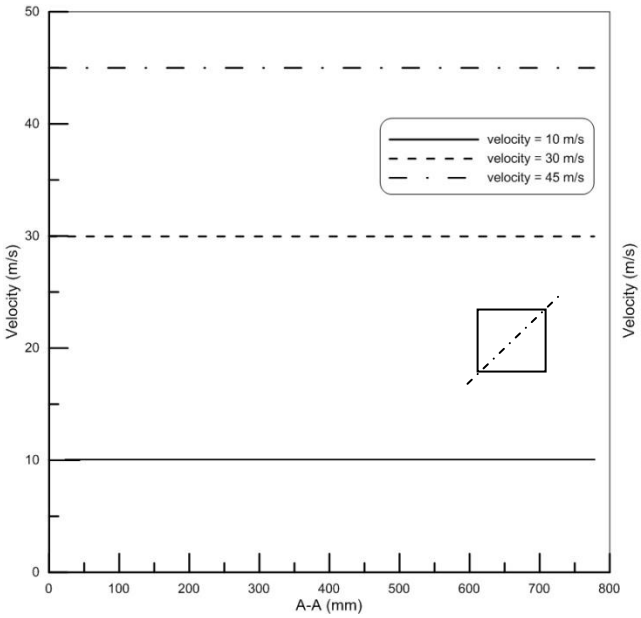

Figure 13. Test section velocity of the diagonal a-a at the inlet plane.

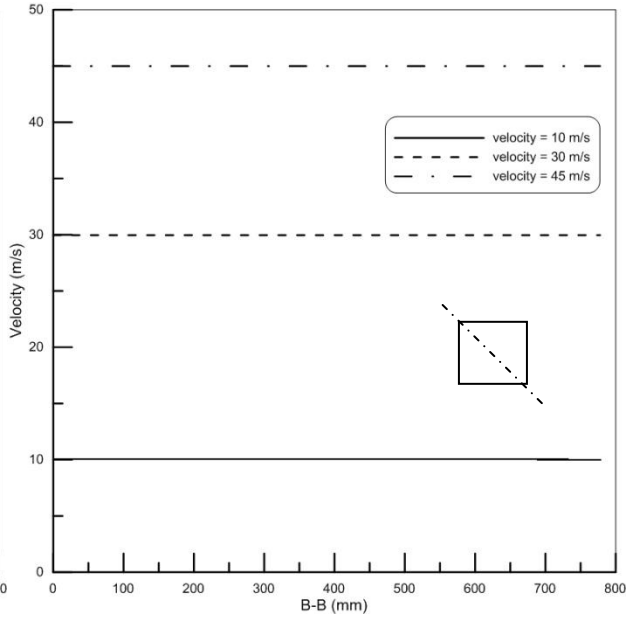

Figure 14. Test section velocity of the diagonal b-b at the inlet plane.

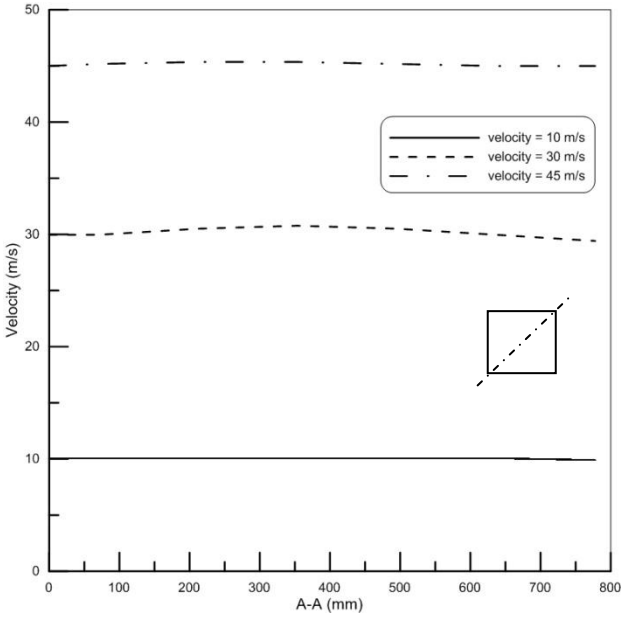

Figure 15. Test section velocity of the diagonal a-a at the mid plane.

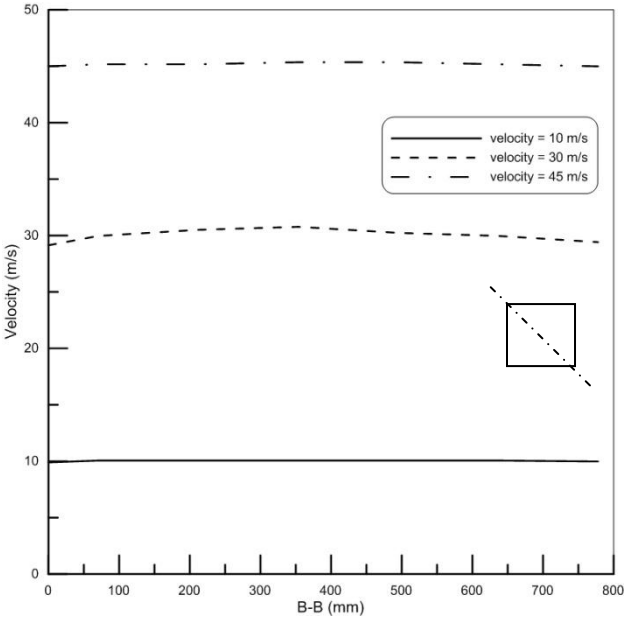

Figure 16. Test section velocity of the diagonal b-b at the mid plane.

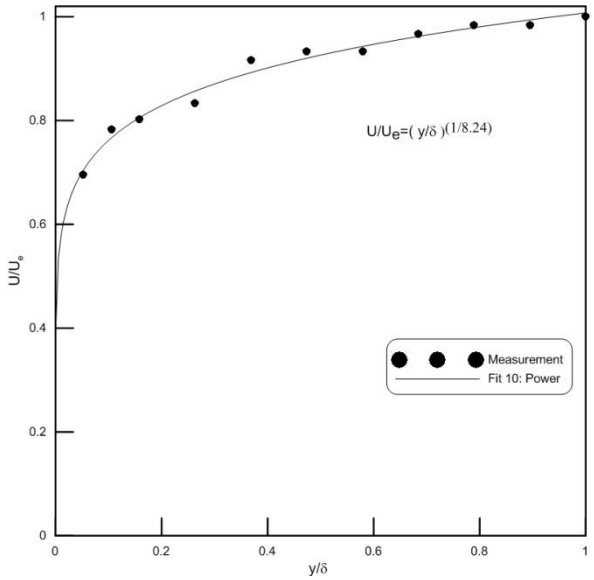

Figure 17. The boundary layer velocity profile over the lower surface of the test section velocity = 10 m/s at mid plane.

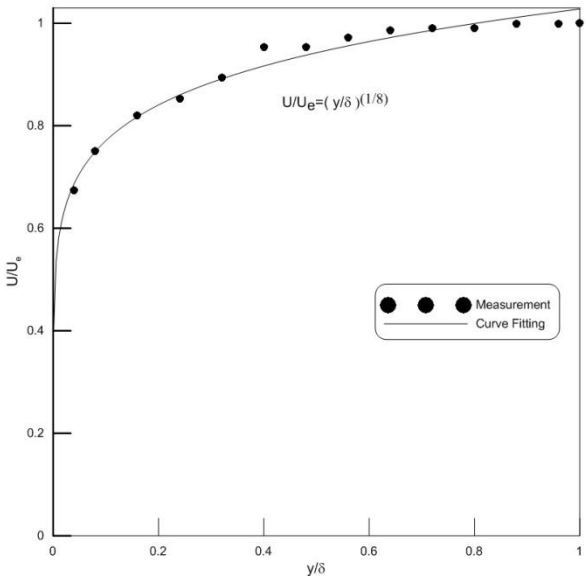

Figure 18. The boundary layer velocity profile over the lower surface of the test section velocity = 30 m/s at mid plane.

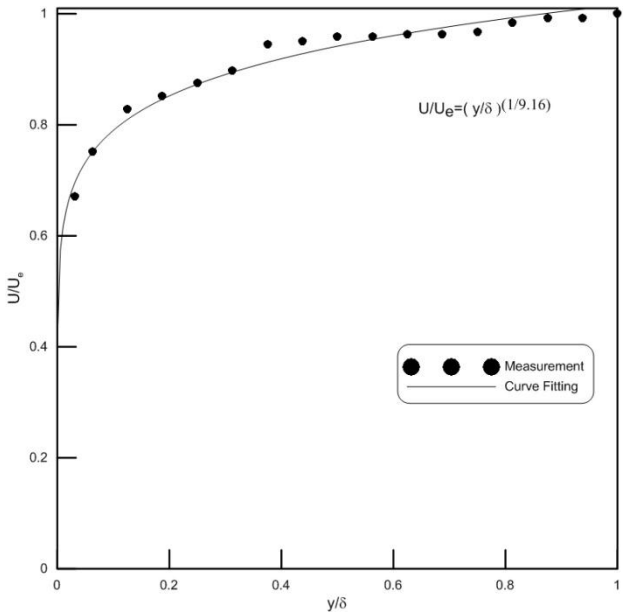

Figure 19. The boundary layer velocity profile over the lower surface of the test section velocity = 45 m/s at mid plane.

Table 1. Boundary layer characteristics inside wind tunnel test section.

Velocity (m/s)	δ (mm)	δ^* (mm)	Θ (mm)	H (mm)
10	19	1.9644E-03	1.58571E-03	0.81
30	25	2.65196E-03	2.12962E-03	0.803
45	32	3.0E-03	2.471E-03	0.82

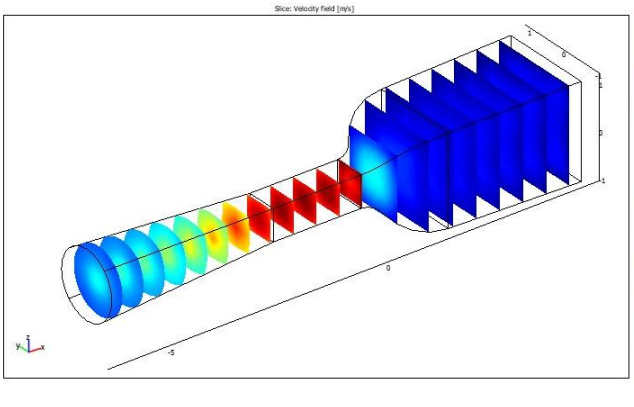

Figure 20. Flow field and pressure simulation inside wind tunnel when inlet velocity 1.23 m/s

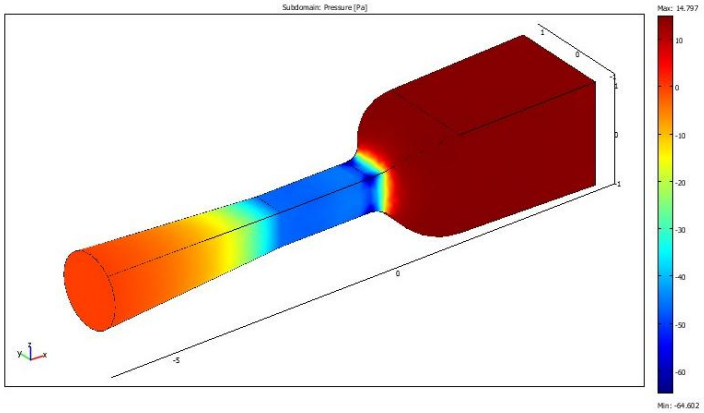

Figure 21. Pressure distribution inside wind tunnel when inlet velocity 1.23 m/s

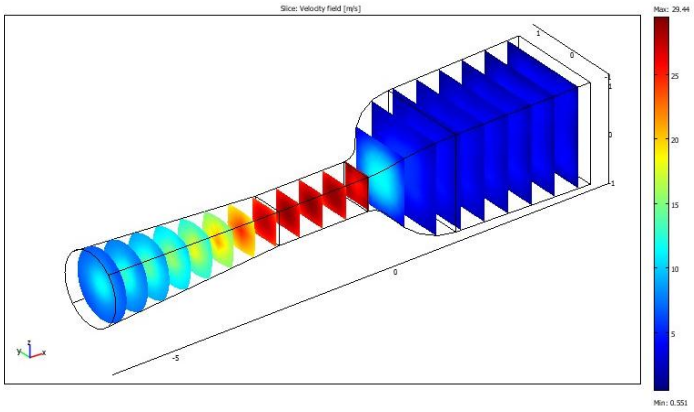

Figure 22. Flow field and pressure simulation inside wind tunnel when inlet velocity 3.5 m/s

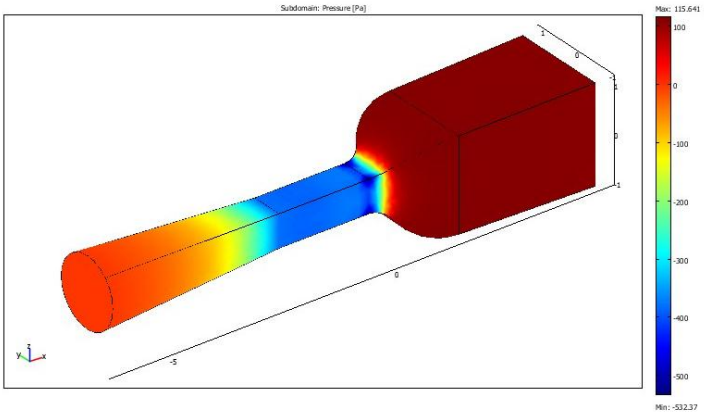

Figure 23. Pressure distribution inside wind tunnel when inlet velocity 3.5 m/s.

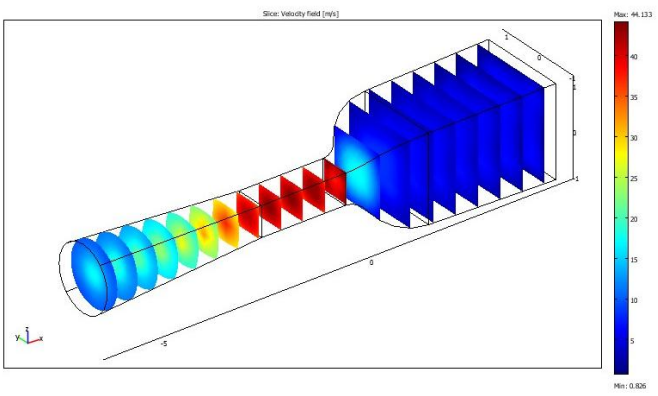

Figure 24. Flow field and pressure simulation inside wind tunnel when inlet velocity 5.25 m/s.

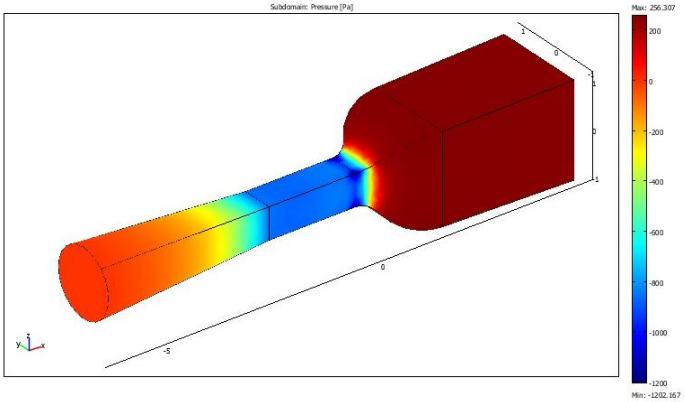

Figure 25. Pressure distribution inside wind tunnel when inlet velocity 5.25 m/s.

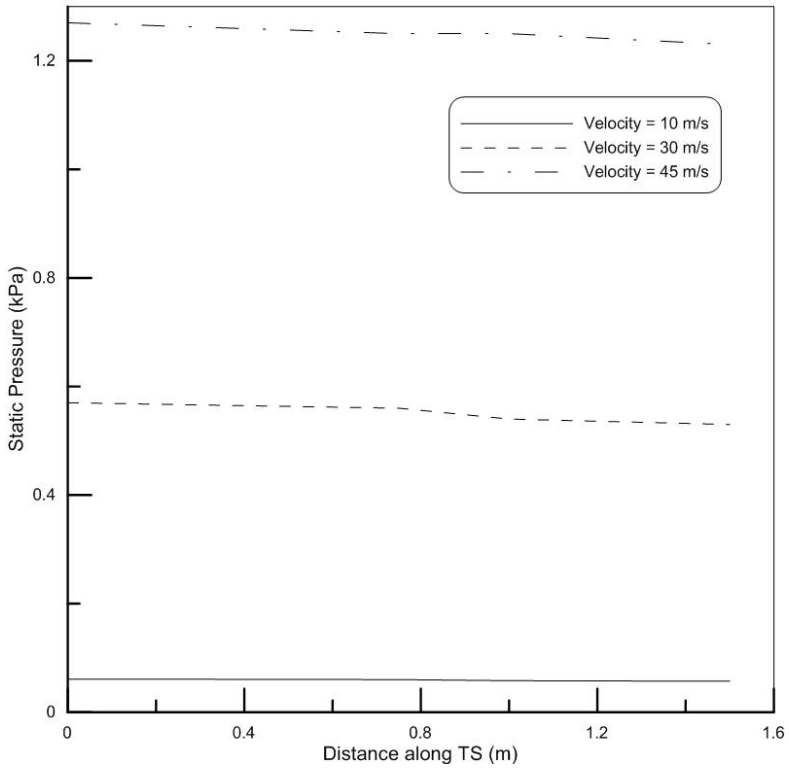

Figure 26. Static pressure along test section for three velocities values.